

Thermal Analysis and Degradation Kinetics of Dextran and Highly Substituted Dextran Acetates

¹ Muhammad Amin, ¹ Muhammad Ajaz Hussain*, ¹ Dure Shahwar, and ² Mazhar Hussain
¹ Department of Chemistry, Ibne Sina Block, University of Sargodha, Sargodha 40100, Pakistan
² Institute of Chemical Sciences, Bahauddin Zakariya University, 60800 Multan, Pakistan
majaz172@yahoo.com*

(Received on 19th May 2015, accepted in revised form 3rd January 2015)

Summary: Dextran acetates were synthesized to study their thermal behavior in comparison with pure dextran. The results have indicated that dextran is significantly stabilized after acetylation. Dextran acetates are thermally 65-74 °C more stable as compared to pure dextran in terms of maximum decomposition temperature ($T_{d,m}$). Likewise, degradation of dextran acetates also starts and ends later than dextran as shown by relatively higher initial (T_d) 3-33 °C and final decomposition temperature (T_d) 55-69 °C. The dextran acetates can be arranged in increasing order of thermal stability: dextran acetate DS 2.91 < dextran DS 2.98 < dextran acetate DS 3. The activation energy (E_a) of dextran and dextran acetates was calculated with the help of Friedman, Broido and Chang kinetic models while order of reaction (n) was calculated from thermal data using Chang and Kissinger models. Several other important parameters were also calculated including frequency factor (Z), enthalpy (ΔH), Gibbs free energy (ΔG) and entropy (ΔS). The integral procedural decomposition temperature (IPDT) and comprehensive index of intrinsic thermal stability (ITS) was also drawn from TG curves using Doyle's method. The dependence of IPDT, ITS and E_a on DS of the acetylation of dextran is also discussed.

Keywords: Decomposition kinetics, Thermodynamics, Dextran acetate, Esterification, Thermostability

Introduction

Dextran is one of the most important biopolymers having broad spectrum of applications in daily life, medicinal and pharmaceutical field [1, 2]. Besides dextran, dextran acetates are also of great commercial interest due to broad spectrum of applications in pharmaceuticals and biomedical fields [3-5]. Polysaccharides have a number of applications in heat resistant coatings and films [6-9]. Therefore, thermal behavior of dextran and its acetates is of great interest due to their commercial applicability.

In spite of utmost importance of the thermogravimetric (TG) behavior of dextran and dextran acetates, there have been few reports on dextran-coated materials [10] where only TG curves were shown. However, none of the reports can address thermal properties and decomposition kinetics of pure dextran and commercially important high loaded dextran acetates, dextran triacetates which signifies the scope of present work.

Our aims are to study thermostability and thermal decomposition kinetics of dextran and highly substituted dextran acetates by using TG, derivative TG (DTG) and second derivative TG (2DTG) analyses. Several important thermogravimetric and thermodynamic parameters, *i.e.*, E_a , n , ITS, IPDT, ΔH , ΔS and ΔG will be drawn from TG analysis and decomposition kinetics.

Experimental

Materials

Dextran (M_w 40000, Fluka) was dried under vacuum at 110 °C for 2 h in order to remove moisture. Other reagents and organic solvents (analytical grade) were acquired from Fluka and used without any further purification. Iodine catalyst was obtained from BDH AnalaR.

Characterization

For FT-IR spectroscopic analysis, pellets with glassy appearance were prepared by trituration of samples with KBr. Before analysis, pellets were dried under vacuum to remove traces of moisture if any, and then spectra were measured on IR Prestige-21 (Shimadzu, Japan). ¹H and ¹³C-NMR spectra of the products were acquired on Bruker 400 MHz NMR machine in deuterated solvents. Thermal degradation of dextran acetates was investigated on SDT Q600 thermal analyzer (TA instruments, New Castle, DE, USA) equipped with Universal Analysis 2000 software v 4.2E. Decomposition was recorded from ambient to 800 °C at 10 °C/min heating rate under nitrogen atmosphere. TG spectral data was exported to MS Excel 2013 and further processed for calculations.

*To whom all correspondence should be addressed.

Acetylation of dextran under solvent free conditions, sample 1, a typical example

Dextran acetates were synthesized as per references [11,12] with slight modification. In this efficient method, iodine (0.5 g; 3.9 mmol) was used as a catalyst and simply dissolved in acetic anhydride (3.49 cm³; 37 mmol). This mixture was added in dried dextran (1.0 g; 6.17 mmol) and refluxed for 3 h at 50 °C. After cooling the reaction mixture to room temperature, saturated aq. sodium thiosulphate solution (cold) was added drop wise to remove excess of iodine from reaction mixture. The precipitates (white) of dextran acetate were filtered off. The sample was vigorously washed with cold distilled water. Dextran acetate was further purified by re-precipitation from acetone into cold distilled water. The product was dried under vacuum at 50 °C overnight. Using same protocol, dextran acetates 2 and 3 were synthesized and purified. Equal amount of iodine as a catalyst was used during all reactions.

Experimental data of sample 1

Yield: 87%; *DS* (degree of substitution): 2.91 (*DS* was calculated by ¹H-NMR spectroscopy); FTIR (KBr, cm⁻¹): 3550 (OH stretching, weak signal), 2930 (CH₂ of sugar units, symmetric and antisymmetric stretching), 1745 (C=O of ester, stretching, strong signal), 1430 (CH₂ of sugar units, scissors vibrations, symmetric stretching), 1032 (C-O-C stretching); ¹H-NMR (400 MHz, CDCl₃, δ / ppm): 3.16-4.89 (anhydroglucose unit), 2.03 (CH₃); ¹³C-NMR (400 MHz, CDCl₃, δ / ppm): 169.67 (-C=O), 20.91 (CH₃), 66.19 (C-6), 70.15 (C-4, C-5), 71.75 (C-2), 73.33 (C-3), 98.26 (C-1).

Experimental data of sample 2

Yield: 92 %; *DS*: 2.98 (*DS* was calculated by ¹H-NMR spectroscopy). FTIR (KBr, cm⁻¹): 3555 (OH stretching, traces), 2939 (CH₂ of sugar units, symmetric and antisymmetric stretching), 1747 (C=O of ester, stretching, strong signal), 1432 (CH₂ of sugar units, scissors vibrations, symmetric stretching), 1038 (C-O-C stretching). ¹H-NMR (400 MHz, CDCl₃, δ / ppm): 3.18-4.91 (anhydroglucose unit), 2.04 (CH₃).

Experimental data of sample 3

Yield: 93%; *DS*: 3.00 (*DS* was calculated by ¹H-NMR spectroscopy). FTIR (KBr, cm⁻¹): 2945 (CH₂ of sugar units, symmetric and antisymmetric stretching), 1747 (C=O of ester, stretching, strong signal), 1433 (CH₂ of sugar units, scissors vibrations, symmetric stretching), 1039 (C-O-C stretching). ¹H-

NMR (400 MHz, CDCl₃, δ / ppm): 3.19-4.91 (anhydroglucose unit), 2.04 (CH₃).

Thermal analysis and degradation kinetics

Decomposition temperatures, *i.e.*, Td_i, Td_m and Td_f were inferred from TG and DTG curves. Friedman, Broido, Chang and Kissinger models were employed for the evaluation of *Ea*. Friedman, Broido, Chang and Kissinger models have been derived from Arrhenius equation and are based on two variables; temperature (*T*) and degree of conversion (*α*). Relation of both these variables is given in eq. 1. Ratio of actual weight loss to the total weight loss (*i.e.*, *α*) is represented in eq. 2. Consequently, the rate of degradation *da/dt* (eq. 3) depends on the temperature and the weight of sample. Eq. 4 is the logarithmic form of eq. 2 used in Friedman method [13]. A straight line graph was obtained by plotting *ln (da/dt)* against 1000/*T* (K⁻¹). Slope (*m*) and intercept (*C*) of the straight line provides values for calculation of *Ea* and *Z*.

$$da/dt = k(T) f(\alpha) \quad (\text{eq. 1})$$

$$\alpha = (W_0 - W_t) / (W_0 - W_\infty) \quad (\text{eq. 2})$$

$$da/dt = Ze^{-Ea/RT} \quad (\text{eq. 3})$$

$$\ln (da/dt) = \ln Z + n \ln (1-\alpha) - Ea/RT \quad (\text{eq. 4})$$

In the method proposed by Broido [14], thermal degradation is always considered to be first order reaction. Equation 5 is used to calculate *Ea* by this method. A graph is plotted between *ln (ln (1/y))* and 1000/*T* (K⁻¹) and *Ea* is calculated from the slope (*m*) of straight line. The Chang method [15] uses eq. 6. Plots are drawn between *ln [(da/dt)/(1-α)ⁿ]* and 1000/*T* (K⁻¹) by changing the value of *n*. Kissinger method [16] is also used for the calculation of order of thermal degradation reaction (*n*). For the calculation of value of *n*, shape index *S* of the DTG curve is quantitatively determined. The expression for *S* is given in eq. 7.

$$\ln (\ln (1/y)) = -Ea/RT + C \quad (\text{eq. 5})$$

$$\ln [(da/dt)/(1-\alpha)^n] = \ln Z - Ea/RT \quad (\text{eq. 6})$$

$$S = [(d^2\alpha/dt^2)_L] / [(d^2\alpha/dt^2)_R] \quad (\text{eq. 7})$$

where, *R* is gas constant and *T* is absolute temperature. Subscript *L* and *R* refer to the values of (*d*²*α/dt*²) at the left and right inflection points of 2DTG curve. Value of *n* was calculated using eq. 8 and 9 as a function of *S* value.

$$n = 1.88S \quad (S \geq 0.45) \quad (\text{eq. 8})$$

$$n = 1.26S^{0.5} \quad (S \leq 0.45) \quad (\text{eq. 9})$$

Thermal stabilities of the dextran and dextran acetates were determined by Doyle's method [17] in terms of integral procedural decomposition temperature (IPDT) and comprehensive index of intrinsic thermal stability (ITS). In this method, both these parameters are evaluated by the areas under TGA curves. The ΔH , ΔS and ΔG were determined by use of standard equations [18, 19].

Results and Discussion

Synthesis and characterization

Dextran acetates with high degree of acetyl substitution were synthesized using efficient, solvent free, one pot and economical reaction methodology as recently adopted [11, 12]. The method produced dextran acetates with high DS 2.91, 2.98 and 3 within 3 h at 50 °C under nitrogen atmosphere. Reactions conditions and results of dextran acetylation are summarized in Table-1. Dextran acetates were purified simply by re-precipitation from acetone in cold water and their purity was verified by FT-IR and ¹H-NMR spectra. Highly pure dextran acetates (**1-3**) were soluble in DMSO, acetone and CHCl₃. It is obvious from results that hydroxyl moieties on dextran were almost completely substituted by acetyl groups.

Table-1: Reaction conditions and results of acetylation of dextran (1.0 g) with I₂ activated acetic anhydride under solvent free conditions.

Sample	Molar ratio ^a	Yield (g, %)	DS ^b	Solubility
1	1:6	2.45, 87	2.91	DMSO, Acetone, CHCl ₃
2	1:9	2.63, 92	2.98	DMSO, Acetone, CHCl ₃
3	1:12	2.66, 93	3.00	DMSO, Acetone, CHCl ₃

^aAGU:acetic anhydride (along with 250 mg I₂ as a catalyst), ^bDS was calculated by ¹H NMR spectroscopy

As the DS is high and products are almost dextran triacetates, therefore, comparable FT-IR absorptions were observed (see experimental data). The most important peak is the strong ester carbonyl absorption which appeared from 1745-1747 cm⁻¹. The FT-IR spectra did not show any hydroxyl group absorptions and presence of strong ester CO signal which are indication of complete acetylation in case of sample **3**. However, some traces of still free OH were observed in sample **1** and **2**.

¹H NMR (δ / ppm, 400 MHz, CDCl₃) spectroscopic analysis has indicated well resolved dextran signals at about 3.16-4.91 ppm. Methyl Hs of acetyl moiety substituted on to dextran appeared at 2.04-2.05 ppm in dextran acetates. The DS of acetylation (Table-1) was also calculated from ¹H-NMR spectra by the comparison of the signal intensities of acetyl vs. anhydroglucose unit-Hs of dextran [20]. ¹³C-NMR (δ / ppm, 400 MHz, CDCl₃) spectrum was also recorded (see experimental data of **3**). The appearance of C=O of dextran acetate at 169.67 ppm confirmed the ester formation between dextran and acetic anhydride. The spectrum has shown signal of CH₃ group of acetyl moiety at 20.91 ppm. The signal for C-6 (CH₂) of dextran appeared at 66.19 ppm. Signals of C-4 and C-5 were overlapped at 70.15 ppm whereas; C-2 and C-3 were found at 71.75 and 73.33 ppm, respectively. C-1 signal appeared further downfield at 98.26 ppm.

Thermal degradation and kinetics

Thermogravimetric curves of dextran and dextran acetates **1-3** were recorded and overlay TG, DTG and 2DTG curves are shown in Figs. 1-3, respectively. The Td_m values for dextran and dextran acetate **1-3** were found 316, 381, 386 and 390 °C, respectively. These Td values have indicated significant stability imparted to dextran after acetylation as Td_m of dextran acetates are 65-74 °C higher than that of pure dextran. Likewise, degradation of dextran acetates also started and ended later as compared to dextran. The Td_i and Td_f appeared 3-33 °C and 55-69 °C higher than that of dextran, respectively. Based on the thermal analysis, dextran acetates can be arranged in increasing order of thermal stability, *i.e.*, dextran < dextran acetate DS 2.91 < dextran DS 2.98 < dextran acetate DS 3.

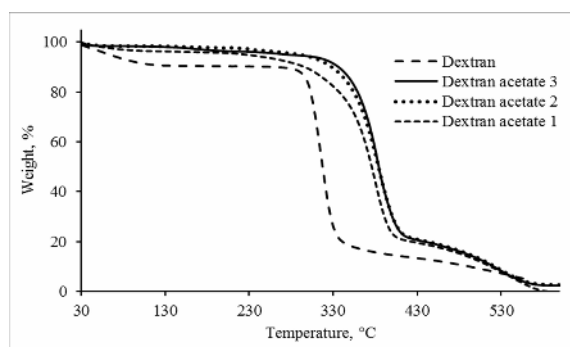


Fig. 1: Overlay TG curves of dextran and dextran acetates.

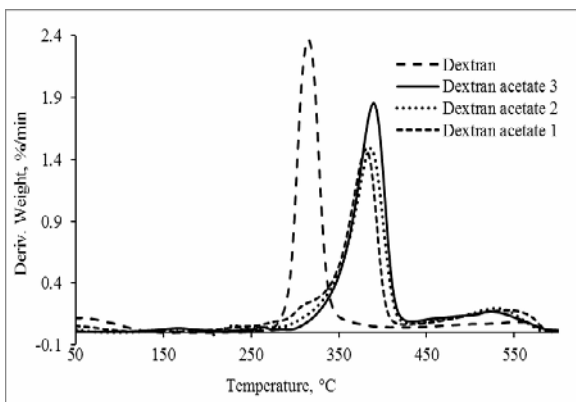


Fig. 2: Overlay DTG curves of dextran and dextran acetates.

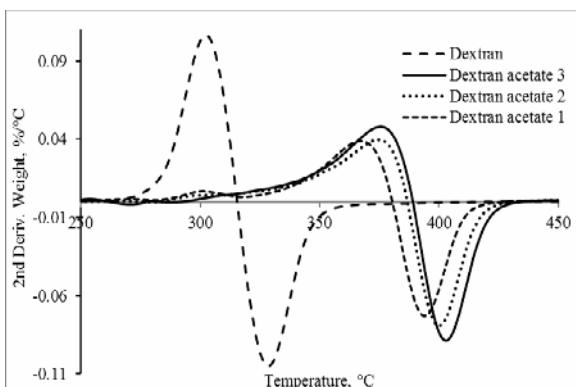


Fig. 3: Overlay 2DTG curves of dextran and dextran acetates.

All dextran acetates 1-3 showed approximately equal weight losses which were in the range of 78.25-78.96% in first degradation step. While, in second step, less than 22 % degradation occurred this may correspond to furfural formation [21] during heating and was not taken into account in present work. The thermal degradation data is summarized in Table-2.

Regarding the calculation of kinetics parameters, four different kinetic models, *i.e.*, Friedman, Broido, Chang and Kissinger were applied on TG data of dextran and dextran acetates 1-3. These models are being widely used for polysaccharide's thermal degradation kinetics [22-25]. Using Friedman, Broido and Chang models, the kinetic parameters like E_a , ΔH , ΔG , ΔS and Z were evaluated. Order of reaction (n) of major thermal degradation step was calculated from Chang and Kissinger models and it was found that degradation followed first order kinetics. The n values have negligible variation with calculating method. Straight

line graphs obtained from Friedman, Broido and Chang models are shown in Figs. 4-6, respectively. E_a was calculated for dextran acetates 1-3 from different kinetic models and found 106-135, 95-113 and 129-139 $\text{kJ}\cdot\text{mol}^{-1}$, respectively which are higher than pure dextran, *i.e.*, 97.28-105.20 $\text{kJ}\cdot\text{mol}^{-1}$. The results of thermal kinetics are summarized in Table-3.

Table-2: Thermal degradation data of dextran and dextran acetates recorded at $10^\circ\text{C}/\text{min}$ in nitrogen.

Sample	T_{d_i} ($^\circ\text{C}$)	T_{d_m} ($^\circ\text{C}$)	T_{d_f} ($^\circ\text{C}$)	Weight loss % at T_{d_f}	Char yield Wt. (%)
Dextran	283.27	315.60	355.87	82.43	4.37 at 565°C
1	286.15	380.77	410.55	78.96	0.25 at 650°C
2	303.35	386.06	419.81	78.28	2.71 at 650°C
3	316.93	389.60	424.46	78.25	1.0 at 650°C

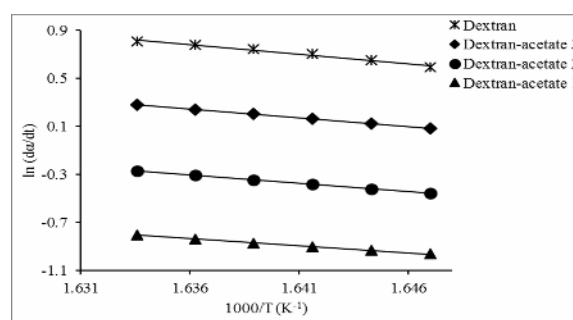


Fig. 4: Friedman graph plotted between $\ln(da/dt)$ and $1000/T$ (K^{-1}) of dextran and dextran acetates.

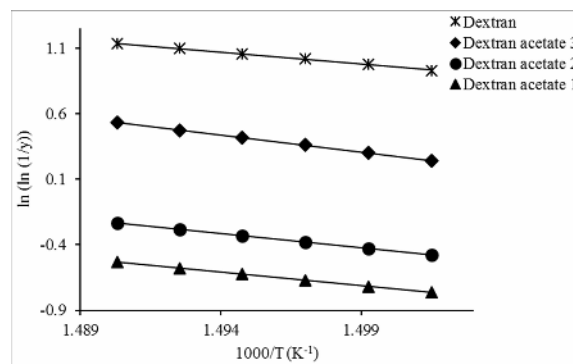


Fig. 5: Broido graph plotted between $\ln(\ln(1/y))$ and $1000/T$ (K^{-1}) of dextran and dextran acetates.

Calculated thermodynamic parameters such as ΔH , ΔS and ΔG from dextran acetates showed relatively higher values compared with those of dextran. The E_a , ΔH , ΔS and ΔG values were found in good agreement with each other for all samples when calculated by different kinetic models.

Table-3: Thermal decomposition parameters and kinetic analysis of dextran and dextran acetates using four kinetic methods.

Sample	Method	r	n	Ea (kJ/mol)	lnA	ΔH	ΔS	ΔG
Dextran	Friedman	0.965	-	97.28	22.15	92.38	81.27	140.26
	Broido	0.996	-	104.35	22.95	99.45	74.46	143.32
	Chang	0.978	1	105.20	24.60	100.30	60.67	136.05
1	Kissinger	-	1.02	-	-	-	-	-
	Friedman	0.998	-	105.94	21.89	100.50	85.76	156.60
	Broido	0.998	-	135.40	26.89	129.95	42.15	157.53
	Chang	0.999	1	126.34	25.06	121.00	57.94	158.80
2	Kissinger	-	1.0	-	-	-	-	-
	Friedman	0.999	-	95.07	18.75	89.59	112.96	164.04
	Broido	0.991	-	112.63	21.02	107.15	92.67	168.23
	Chang	0.999	1	106.71	19.92	101.23	102.27	168.64
3	Kissinger	-	0.94	-	-	-	-	-
	Friedman	0.999	-	129.08	26.65	123.57	44.88	153.33
	Broido	0.989	-	136.16	27.13	130.64	40.45	157.47
	Chang	0.999	1	138.62	27.78	133.11	34.89	156.24
	Kissinger	-	1.02	-	-	-	-	-

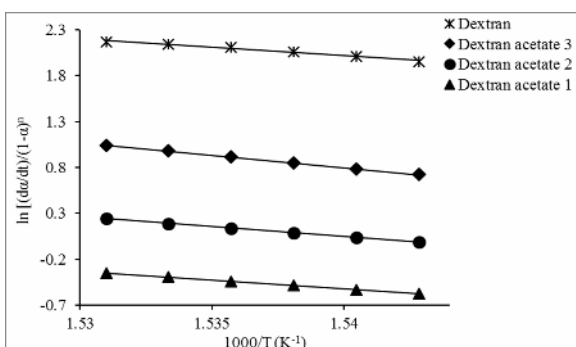


Fig. 6: Chang graph plotted between $\ln [(da/dt)/(1-a)^n]$ and $1000/T (K^{-1})$ of dextran and dextran acetates.

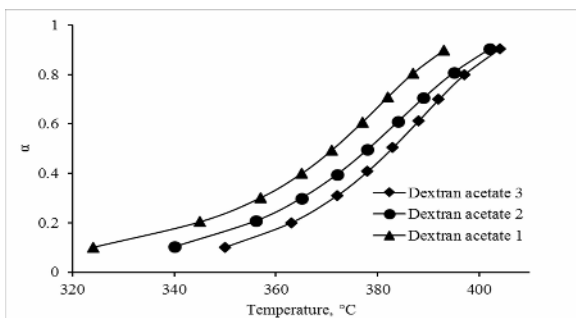


Fig. 7: A plot between α and temperature for dextran acetates.

The ITS and IPDT values for dextran acetates 1-3 were found to be in the range 0.56-0.61 and 361.40-385.76 °C, respectively which are indicative of good thermal stability of the materials. Degree of conversion (α) as well as weight loss (%) vs. temperature were plotted for dextran acetates 1-3 and presented in Fig. 7 and 8, respectively to further clarify their relation. We have also tried to establish the relationship of DS with IPDT and ITS values. The results have indicated that among dextran

acetates, dextran triacetate (DS 3) has highest IPDT value (385.76) than dextran (321.52) and other dextran acetates with DS 2.91 and 2.98 (Fig. 9). Its of all samples were also calculated and similar trend like IPDT was observed (Fig. 10). Therefore, it is concluded that both IPDT and ITS values are increased with increasing degree of acetylation indicated that stability is imparted to dextran after acetylation.

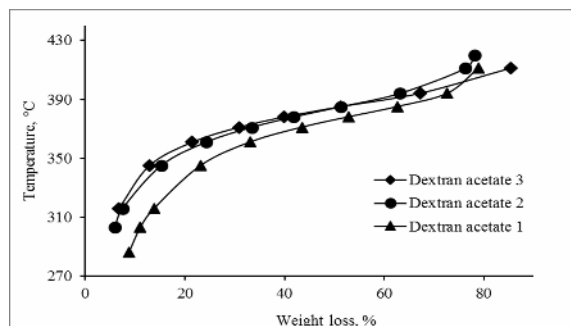


Fig. 8: A Plot between weight loss % and temperature for dextran acetates.

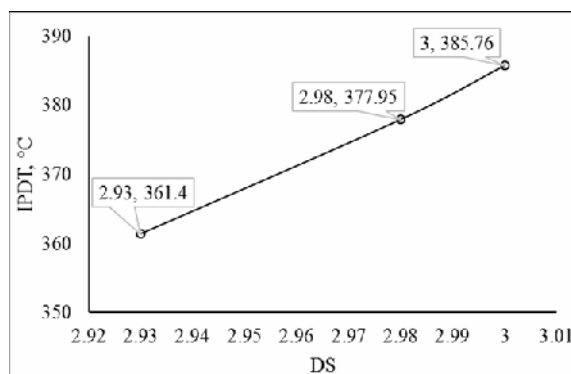


Fig. 9: A plot between IPDT and DS for dextran acetates 1-3 showing increasing thermal stability with increasing degree of substitution.

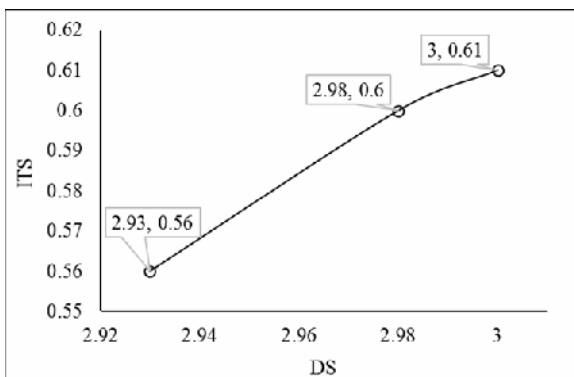


Fig. 10: A plot between ITS and DS for dextran acetates 1-3 showing increasing thermal stability with increasing degree of substitution.

Conclusions

Highly substituted dextran acetates with enhanced thermal stability were fabricated with higher thermal degradation temperature maxima as compared to dextran polymer. The extra stability of dextran acetates was also inferred from higher values of kinetic and thermodynamic parameters. Important thermal parameters, *i.e.*, IPDT and ITS values, indicated that dextran acetates are thermally more stable entities as compared to unmodified dextran. It is also concluded that among dextran acetates, triacetates are the thermally most stable materials. Such thermally stable and economically produced dextran acetates could be potential materials for heat resistance and biomedical applications.

References

1. T. Heinze, T. Liebert, B. Heublein and S. Hornig, Functional Polymers Based on Dextran, *Adv. Polym. Sci.*, **205**, 199 (2006).
2. D. Stanić-Vučinić and T. Č. Veličković, The Modifications of Bovine β -lactoglobulin Effects on its Structural and Functional Properties, *J. Serb. Chem. Soc.*, **78**, 445 (2013).
3. J. Qi, P. Yao, F. He, C. Yu and C. Huang, Nanoparticles with Dextran/Chitosan Shell and BSA/Chitosan Core-Doxorubicin Loading and Delivery, *Int. J. Pharm.*, **393**, 176 (2010).
4. V. Vlies, A. J. Han, W. Hiroshi and U. J. Hasegawa, Dextran Acetate-Based Sponge as Cell Scaffold for Tissue Engineering, *J. Biomater. Tissue Eng.*, **4**, 28 (2014).
5. M. Beesh, P. Majewska and Th. F. Vandamme, Synthesis and Characterization of Dextran Esters as Coating or Matrix Systems for Oral Delivery of Drugs Targeted to the Colon, *Int. J. Drug Delivery.*, **2**, 22 (2010).
6. X. Q. Nguyen, M. Sipek, V. Hynek and Q. T. Nguyen, Flow Method for Study of Gas Transport in Polymers. Application to the Study of Oxygen, Nitrogen, and Carbon Dioxide Permeation Through Cellulose Acetate Membranes. *J. Appl. Polym. Sci.*, **54**, 1817 (1994).
7. O. Carp, L. Patron, D. C. Culita, P. Budrugaec, M. Feder and L. Diamandescu, Thermal Analysis of Two Types of Dextran-Coated Magnetite, *J. Therm. Anal. Calorim.*, **101**, 181 (2010).
8. G. Számel, S. Klébert, I. Sajó and B. Pukánszky, Thermal Analysis of Cellulose Acetate Modified with Caprolactone, *J. Therm. Anal. Calorim.*, **91**, 715 (2008).
9. L. Cabrales and N. Abidi, On the Thermal Degradation of Cellulose in Cotton Fibers, *J. Therm. Anal. Calorim.*, **102**, 485 (2010).
10. M. A. Hussain, D. Shahwar, M. N. Tahir, M. Sher, M. N. Hassan and Z. Afzal, An Efficient Acetylation of Dextran Using *in Situ* Activated Acetic Anhydride with Iodine, *J. Serb. Chem. Soc.*, **75**, 165 (2010).
11. A. Juríková, K. Csach, J. Miškuf, M. Koneracká, V. Závišová, M. Kubovčíková and P. Kopčanský, Thermal Analysis of Magnetic Nanoparticles Modified with Dextran, *Acta. Phy. Pol. A.*, **121**, 1296 (2012).
12. M. A. Hussain, D. Shahwar, M. N. Hassan, M. N. Tahir, M. S. Iqbal and M. Sher, An Efficient Esterification of Pullulan Using Activated Carboxylic Acid Anhydrides with Iodine, *Collect. Czech. Chem. Commun.*, **75**, 133 (2010a).
13. H. L. Friedman, Kinetics of thermal degradation of char-forming plastics from thermogravimetry. Application to a phenolic plastic, *J. Polym. Sci. Part C*, **6**, 183 (1963).
14. A. Broido, A simple, sensitive graphical method of treating thermogravimetric analysis data, *J. Polym. Sci. Part A-2 Polym. Phys.*, **7**, 1761 (1969).
15. W. L. Chang, Decomposition behavior of polyurethanes via mathematical simulation, *J. Appl. Polym. Sci.*, **53**, 1759 (1994).
16. H. E. Kissinger, Reaction kinetic in differential thermal analysis, *Anal. Chem.*, **29**, 1702 (1957).
17. C. D. Doyle, Estimating thermal stability of experimental polymers by empirical thermogravimetric analysis, *Anal. Chem.*, **33**, 77 (1961).
18. A. M. Adel, Z. H. A. El-Wahab, A. A. Ibrahim and M. T. Al-Shemy, Characterization of

- microcrystalline cellulose prepared from lignocellulosic materials. Part I. Acid catalyzed hydrolysis, *Bioresour. Technol.*, **101**, 4446 (2010).
19. M. Ghaemy and S. M. A. Nasab, Synthesis and identification of organosoluble polyamides bearing a triaryl imidazole pendent: thermal, photophysical, chemiluminescent, and electrochemical characterization with a modified carbon nanotube electrode, *React. Funct. Polym.*, **70**, 306 (2010).
 20. T. Heinze, T. Liebert, K. S. Pfeiffer and M. A. Hussain, Unconventional cellulose esters: synthesis, characterization and structure–property relations, *Cellulose*, **10**, 283 (2003).
 21. M. S. Iqbal, J. Akbar, S. Saghir, A. Karim, A. Koschella, T. Heinze and M. Sher, Thermal studies of plant carbohydrate polymer hydrogels, *Carbohydr. Polym.*, **86**, 1775 (2011).
 22. M. S. Iqbal, J. Akbar, M. A. Hussain, S. Saghir and M. Sher, Evaluation of hot-water extracted arabinoxylans from ispaghula seeds as drug carriers, *Carbohydr. Polym.*, **83**, 1218 (2011).
 23. M. A. Hussain, K. Abbas, M. Amin, B. A. Lodhi, S. Iqbal, M. N. Tahir, W. Tremel. Novel high-loaded, nanoparticulate and thermally stable macromolecular prodrug design of NSAIDs based on hydroxypropylcellulose, *Cellulose*, **22**, 461(2015).
 24. A. Abbas, M. A. Hussain, M. Amin, R. N. Paracha, M. Ameer and M. Hussain, Green Synthesis, Thermal Analysis and Degradation Kinetics of Cross-Linked Potato Starch, *J. Chem. Soc. Pak*, **37**, 277 (2015).
 25. M. A. Hussain, A. Zarish, K. Abbas, M. Sher, M. N. Tahir, W. Tremel, M. Amin, A. Ghafoor and B. A. Lodhi, Hydroxypropylcellulose-aceclofenac conjugates: high covalent loading design, structure characterization, nano-assemblies and thermal kinetics, *Cellulose*, **20**, 717 (2013).